Processing, structure and mechanics of fibres of heteroaromatic oxazole polymers

M. E. Hunsaker
Polymer Branch, Air Force Materials Laboratory, Wright-Patterson AFB, Ohio 45433, USA

and G. E. Price and S. J. Bai*
Research Institute, University of Dayton, Dayton, Ohio 45469, USA
(Received 9 October 1990; accepted 4 February 1991)

Fibres of the rod-like molecule poly-*p*-phenylene benzobisoxazole (PBO) and the coil-like molecule poly-2,5-benzoxazole (ABPBO) were spun from polymerization dopes and then coagulated at various temperatures. Axial tension was applied in drying the coagulated wet filaments; heat treatment was applied to anneal the fibres. Wide-angle X-ray scattering on the fibres revealed that tension drying improved molecular alignment leading to increased tensile modulus. Small-angle X-ray scattering (SAXS) showed that the void content of the fibres was significantly reduced by low coagulation temperature, tension drying and thermal annealing. This reduction of voids also contributed to enhanced tensile properties. Thermal annealing also improved the crystallinity of the ABPBO fibres and seemed to induce a three-dimensional order, which was usually absent for fibres of the rod-like PBO polymer. Both annealed PBO and ABPBO fibres resulted in a unique off-axis radial four-point SAXS pattern. The tensile modulus for fibres of the rod-like polymer was higher than that of the coil-like polymer. However, as determined by the cantilever beam test, the critical compressive strain for fibres of the rod-like polymer was lower than that of the coil-like polymer.

(Keywords: poly-*p*-phenylene benzobisoxazole; poly-2,5-benzoxazole; liquid crystalline polymers; fibres; tensile properties)

INTRODUCTION

Heterocyclic aromatic polymers[1–9] have been under development for their inherently superior thermo-oxidative stability and solvent resistance. Improved mechanical strength, high ballistic properties and gain in processing advantages have been realized for these heteroaromatic polymers with high molecular weight. They are considered to be cost-effective replacements for aromatic and aliphatic polyamide polymers as engineering fibres or as the reinforcing component in structural composites. More recently, they have been used in molecular composites[10,11] as the reinforcing molecule and the matrix molecule.

The focus of previous studies on heteroaromatic polymers has been on poly-*p*-phenylenebenzobisthiazole (PBT). PBT is one of the heteroaromatic polymers commonly called PBX, as sketched in *Figure 1*, which assumes a *para*-catenated backbone. This gives a rod-like polymer. The only conformational flexibility is provided by the rotation of bonds between alternating phenylene and heterocyclic groups[12,13]. As a result of its rigidity, this type of rod-like molecule generally forms a nematic liquid-crystalline phase. Another group of heteroaromatic polymers is given a generic name of ABPBX, as illustrated in *Figure 1*, which assumes an extended-chain configuration and can also form a liquid-crystalline phase. This characteristic becomes of considerable interest, since fibres and films from these liquid-crystalline polymers can have both superior mechanical properties and thermal stability. Most heteroaromatic polymers do not exhibit glass transition behaviour before thermal degradation at above 560°C and are soluble only in few protic acids. These factors rule out conventional thermal molding or extrusion to be applied for processing these polymers. Instead, the polymers are generally processed by coagulation from an acid solution.

The heteroaromatic polymers in solution tend to exhibit lyotropic liquid-crystalline characteristics, i.e. the solution morphology will change from isotropic to anisotropic (nematic) by increasing polymer concentration. This greatly influences the intermolecular arrangement of the molecules in solution, and thus has a deterministic effect in the final structure and properties of the articles made from the polymers. The coagulation scheme induces drastic dimensional and morphological changes. One of the dominant effects is certainly the formation of voids. Significant success has been achieved in extrusion of PBX or ABPBX fibres directly from a nematic polymerization reaction mixture in polyphosphoric acid (PPA) followed by coagulation in a non-solvent. A broad database has been established for understanding the synthesis chemistry, solution characteristics, processing conditions, mechanical properties and morphology of fibres spun from the polymerization mixture in PPA. Lately processing–property efforts concerning PBX fibres have been focused on increasing the tensile modulus and compressive strength through enhancement of intermolecular interactions, while minimizing defects through reduction of voids.

The success in synthesizing related heteroaromatic

* To whom correspondence should be addressed

0032-3861/92/102128-08

ROD

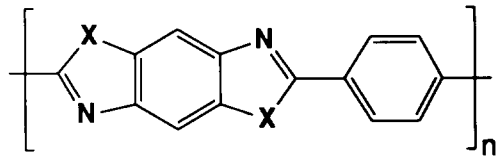

PBX

X = O *(cis)*	POLY-P-PHENYLENE BENZOBISOXAZOLE	**PBO**
X = S *(trans)*	POLY-P-PHENYLENE BENZOBISTHIAZOLE	**PBT**
X = NH	POLY-P-PHENYLENE BENZOBISIMIDAZOLE	**PBI**

COIL

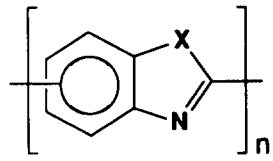

ABPBX

X = O	POLY-2,5-BENZOXAZOLE	**ABPBO**
X = S	POLY-2,6-BENZTHIAZOLE	**ABPBT**
X = NH	POLY-2,5(6)-BENZIMIDAZOLE	**ABPBI**

Figure 1 Chemical structures of PBX and ABPBX molecules

polymers of high molecular weight by J. Wolfe of SRI International, Menlo Park, CA, led to the availability of two promising polymers: poly-*p*-phenylenebenzobisoxazole (PBO), a rod-like polymer, and poly-2,5-benzoxazole (ABPBO), an extended-chain molecule (*Figure 1*). A preliminary effort in spinning PBO and ABPBO polymers produced fibres with properties superior to those of PBT fibre and with interesting morphological features. Further studies of processing, structure, as well as mechanics of PBO and ABPBO fibres were begun.

Here, the results of correlating processing conditions, microstructure and mechanical properties of PBO and ABPBO fibres are reported. The objective of this study was to relate a reduction in void content and increase in molecular orientation with the improvement of mechanical properties. Two different processing approaches were employed to achieve this objective. In the first, the effects of influencing fibre structure through different coagulation temperatures and drying conditions were studied. In the second, heat treatment conditions were varied to determine their effects on mechanical properties. Tensile and compressive properties of single filaments from these two approaches are presented in this paper, along with the microstructure determined by scanning electron microscopy and by X-ray scattering.

PROCESSING OF FIBRES

A PBO polymer of $[\eta] = 17.1\ \mathrm{dl\ g^{-1}}$ was obtained in PPA as a polymerization mixture with PBO weight fraction of 9.9%; and an ABPBO polymer of $[\eta] = 17.5\ \mathrm{dl\ g^{-1}}$ was obtained, also in PPA, as a polymerization mixture with ABPBO weight fraction of 16.9%. The intrinsic viscosity $[\eta]$ was measured in methanesulphonic acid at 30°C. The heteroaromatic oxazole polymers were synthesized by polycondensation in PPA to high molecular weight and were provided by J. Wolfe.

Monofilaments of PBO and ABPBO were extruded by dry-jet, wet spinning the polymerization mixtures. The nematic liquid-crystalline solutions were heated, extruded isobarically through a 0.025 cm diameter spinneret at a spin draw ratio of 69, and coagulated in distilled water.

The first approach in changing post-spinning conditions was by varying the coagulation temperature. Fibres were spun as described, then coagulated in distilled water at 11, 24 and 40°C. This was designed to investigate the structure and properties of the fibres as a function of coagulation temperature. After rinsing to remove residual acid, the fibre was dried with and without tension. Two tension-drying schemes were applied here. In the first, a tensile strain of 0.015 ± 0.005 was imposed on the wet filament by using a stretcher, and then air-dried at room temperature. In the second, the wet filament was fed through a tube furnace at 90°C, and a tensile strain of 0.015 ± 0.003 was applied by controlling the differential speed of fibre-feeding and take-up. A fibre sample coagulated at 24°C and tension-dried by the second scheme was further heat treated at 500°C to study changes in properties and morphology due to thermal annealing.

In the second approach, heat treatment was employed on selected fibre specimens. The monofilaments were annealed in the tube furnace set at 300, 415 and 510°C in a dried nitrogen atmosphere. It was reported that the

properties and the structure of this type of fibres were insensitive to the duration of heat treatment[14]. For this study, a resident time of 0.5 min was used for annealing the fibres. A tensile strain of 0.015 ± 0.002 was maintained during the course of thermal annealing by controlling the differential speed. Other PBO and ABPBO fibres were similarly annealed at 430°C with varying tensile strains from 0.014 up to 0.064 for properties and microstructure investigations.

MECHANICAL PROPERTIES

Tensile properties, including Young's modulus E_t, tensile strength σ_t, and strain at break ε_b, were determined for the PBO and ABPBO fibres following ASTM Procedure D3379 for high-modulus filament. Single filament was mounted on a pre-cut manila tab with 2.54 cm (one inch) gauge length by using fast-setting epoxy glue. Tensile deformation was applied with an Instron tester using a 200 g load cell and a deformation rate of 0.05 cm min^{-1}. The diameter of each filament was measured by a split-image microscope. Because of the dry-jet, wet-spinning and coagulation scheme used for extruding fibres from the heterogeneous and nematic solutions, variations in fibre diameter were observed. Examinations along several cross sections of each specimen were made, and the averaged diameter was used for calculating cross section area A and tensile stress. For each fibre, multiple specimens were tested. The testing results were used inclusively for calculating the averaged tensile properties. Young's modulus E_t was further corrected for machine compliance:

$$E_t = L/[(C_a - C_s)A] \quad (1)$$

the detection medium for the X-ray measurements. This permits direct comparison of the scattering intensities to strength σ_t was calculated from the load at break divided by A. Tensile properties of the PBO and the ABPBO fibres are listed in *Tables 1–3*.

Several fibre testing schemes[15–19] for axial compressive strength were investigated. Cantilever beam testing[19] was chosen for its simplicity and for requiring just a small amount of fibre. Single filaments were attached to a Lucite beam by means of a thin coating of acrylic spray. Axial compression was applied to the fibre when the cantilever beam was bent, as shown in *Figure 2*. The formation of kink bands and/or slip planes along the fibre was considered to indicate compressive failure. The

Table 1 Tensile properties of tension-dried PBO fibres coagulated at different temperatures

PBO fibre	d_0 (μm)	E_t (GPa)	σ_t (GPa)	ε_t (%)
11°C[a]	31 ± 5	70	2.0	7.0
Tensile dried[b]	28 ± 3	172	2.3	3.1
24°C[a]	23 ± 3	76	2.4	7.0
Tensile dried[b]	20 ± 3	82	2.3	6.2
and heat treated at 500°C	23 ± 5	103	1.8	2.4
41°C[a]	23 ± 3	76	1.4	3.4
Tensile dried[b]	23 ± 5	145	1.9	4.0

[a]Coagulation bath temperature
[b]Tensile strain of 0.015 applied on the wet filament

Table 2 Mechanical properties of heat-treated PBO fibres

PBO fibre	d_0 (μm)	E_t (GPa)	σ_t (GPa)	ε_b (%)	ε_c[a] (%)	σ_c[a] (GPa)
Room temperature as-spun fibre	30 ± 2	87	3.1	6.6	0.19	0.17
With strain of 1.5%[b]						
Heat treated at 300°C	28 ± 8	115	2.6	3.6	0.18	0.21
Heat treated at 415°C	28 ± 8	137	2.6	3.6	0.19	0.26
Heat treated at 510°C	27 ± 7	172	2.4	2.9	0.17	0.29
Heat treated at 430°C with strain of:						
1.4%[b]	25 ± 2	191	3.6	3.2		
2.9%[b]	28 ± 1	251	3.1	2.5		
6.0%[b]	22 ± 1	285	2.9	3.6		

[a]Cantilever beam test
[b]Tensile strain applied during heat treatment

Table 3 Tensile properties of ABPBO fibres

ABPBO fibre	d_0 (μm)	E_t (GPa)	σ_t (GPa)	ε_b (%)
Room temperature as-spun fibre	33 ± 8	72	3.1	7.0
With strain of 1.5%[a]				
Heat treated at:				
300°C	43 ± 3	88	1.4	4.1
415°C	48 ± 8	96	1.9	4.0
510°C	56 ± 8	108	1.3	4.2
Heat treated at 430°C with strain of:				
1.4%[a]	41 ± 8	83	2.5	6.4
3.3%[a]	33 ± 5	106	3.4	7.0
6.4%[a]	31 ± 8	212	2.4	2.7

[a]Additional tensile strain applied during heat treatment

CANTILEVER BEAM BENDING TEST

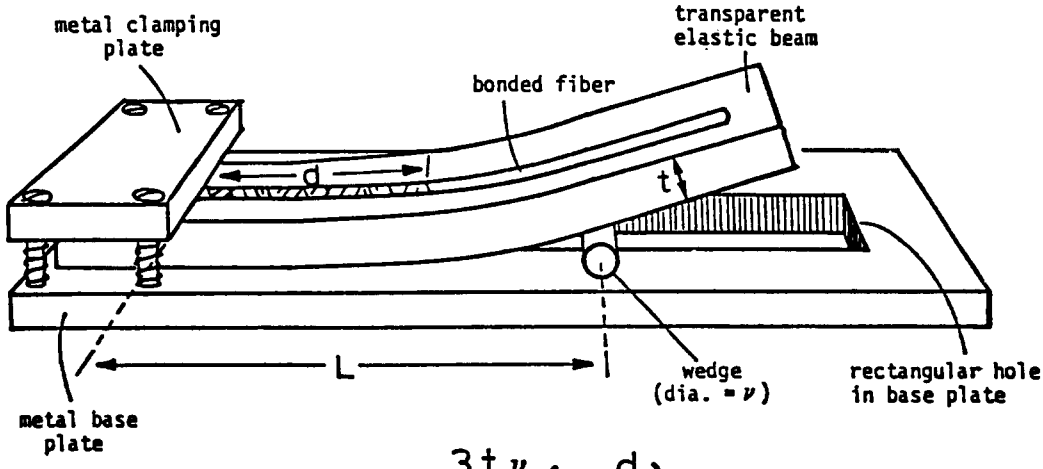

Figure 2 Schematic illustration for cantilever beam test

Table 4 Critical compressive strain of single filament measured by cantilever beam test

Fibre	E_t (GPa)	ε_c (%)
PBO as-spun fibre	87	0.19 ± 0.02
Heat treated at:		
300°C	115	0.18 ± 0.03
415°C	137	0.19 ± 0.04
500°C	172	0.17 ± 0.02
PBT as spun-fibre	180	0.19 ± 0.04
Heat treated at 650°C	261	0.20 ± 0.02
ABPBO heat treated at 525°C	130	0.42 ± 0.04
Kevlar 49	130	0.57 ± 0.02

maximum distance of kink band from the fixed end was located by using an optical microscope, and used for calculating critical compressive strain ε_c, which was then corrected for the prestrain in mounting the filament. With the assumption that (1) tensile and compressive moduli are equal, (2) the compressive deformation is elastic and (3) the failure mechanism is identical for the fibres, the critical compressive strength σ_c of the fibre can be obtained as

$$\sigma_c = E_t \varepsilon_c \quad (2)$$

For each filament, multiple compressive failures could be induced by bending the cantilever beam to different degrees; and for each fibre, several filaments were tested. The averaged results are listed in *Tables 2* and *4*. Since the validity of assumptions (1)–(3) for our PBO and ABPBO fibres has not been completely demonstrated, the results of σ_c, unlike ε_c, should be considered as reference values only. In addition, the fibre compressive properties will be compared with those obtained from direct compression of the fibres[18]. For fibres inherently having kink bands or slip planes, this testing scheme is not applicable and no compressive properties were measured.

For purposes of comparison, fibres of PBT and Kevlar 49 were similarly tested for tensile modulus and critical compressive strain. The results are compiled in *Table 4*.

SCANNING ELECTRON MICROSCOPY

A scanning electron microscope (SEM) was used to image both tensile and freeze-fractured (at −195°C) cross sections of the fibres for examining fracture behaviour and skin–core differentiation. An Alpha 9 SEM with a design resolution of 12 nm distributed by International Scientific Instruments, Inc. was used. Fibre specimens were sputter coated with Au:Pd to enhance imaging contrast. SEM images were recorded on Polaroid P/N 55 film.

X-RAY SCATTERING

For X-ray scattering measurements on the uniaxially oriented systems, a flat-film camera with pin-hole collimation was used. The X-ray source was Cu Kα radiation from a Rigaku RU-300 rotating-anode generator with a graphite crystal as the monochromator. Each fibre specimen was wound along the fibre axis to form a bundle that was attached vertically onto the exit of the collimator; the convention of designating equatorial (horizontal) and meridional (vertical) reflections applies here. Variations in the sample–film distance enabled performance of both wide-angle X-ray scattering

(WAXS) and small-angle X-ray scattering (SAXS) measurements.

For this study the WAXS covered a reciprocal space of $40 > Q > 4\ nm^{-1}$, where $Q = 4\pi \sin(\theta/2)\lambda$, where λ is the wavelength and θ the scattering angle. This allows coverage of a real space range, d, of $0.16 < d < 1.57$ nm, which is most relevant to the unit cell structure, lattice orientation and molecular packing. The SAXS covered a reciprocal space range of $6.0 > Q > 0.2\ nm^{-1}$, or equivalently $1.0 < d < 31$ nm, which is related to collective arrangement of crystallites and defects (voids) of the fibres and thus more related to the mechanical properties.

The intensity of [001] reflection, which is along the meridional direction, is proportional to the amount of repeat unit of the polymers in the uniaxially oriented fibres. This reflection was used as an internal standard to normalize the scattering intensities to account for variances in the radiation source, the fibre amount and the detection medium for the X-ray measurements. This permits direct comparison of the scattering intensities to correlate more precisely the microstructure, properties and processing conditions. X-ray scattering intensities were registered on Osray films and digitized by a Joyce-Loebl Scandig 3 microdensitometer. The digitized intensities were then processed by computer codes to generate contour plots and line scans for analyses.

RESULTS AND DISCUSSION

As represented in *Tables 1–4*, the correlation of processing parameters and the mechanical properties clearly demonstrates the following points.

(1) All the dry-jet, wet-spun PBO and ABPBO fibres had significant variation in their diameter d_0. This was expected and had been reported before for laboratory-scale processing of fibres via the spinning and coagulation technique. The exothermic diffusion and the non-equilibrium hydrodynamic behaviour existing in the coagulation of the polymer are believed to cause a continuously changing coagulation environment around the extruded filament, which contributed to variations in fibre diameter. This in turn will produce variation in cross section area and in the mechanical properties. It is then necessary to test an adequate ensemble of fibre specimens for reliable mechanical properties.

(2) As-spun PBO fibres coagulated in water of different temperatures, from 11 to 41°C, showed no difference in tensile modulus, but a distinctly lower tensile strength for the fibre coagulated in 41°C water (cf. *Table 1*). This might be due to the diffusion mechanism involved in coagulating the fibres. Upon coagulation, the fibres extruded from polymerization mixtures containing less than 18 wt% of polymer would undergo a volumetric reduction in leaching out the solvent. At a higher coagulation bath temperature, the coagulation or diffusion rate would become faster, leading to a more drastic dimensional shrinkage, a larger degree of void formation and thus a lower tensile strength for the fibre.

(3) Tensile moduli of the PBO and the ABPBO fibres could be greatly enhanced either by drying under tension or by thermal annealing. Drying with a larger tensile strain or annealing at a higher temperature consistently gave an improved tensile modulus as shown in *Tables 1–3*. The two tension-drying schemes outlined before produced similar results. However, tensile strength of the PBO and the ABPBO fibres was insensitive to the drying tensions or the annealing temperatures.

(4) The critical compressive strain ε_c of PBO or ABPBO fibres was constant within our processing window. The improvement in critical compressive strength, as determined by the cantilever beam test, could be attributed mainly to the increase in tensile modulus. This result is interesting and intriguing. Results of direct compression of a different heat-treated PBO monofilament[18] showed the tensile modulus and compressive modulus to be close in value, and the compressive strength to be similar to that obtained here for the PBO fibres from using the cantilever beam test. Since kink-band formation was observed and considered to indicate critical compressive failure in both the direct compression test and the cantilever beam test, similar compressive strength results from these two tests suggest that PBO fibres show kink-band formation in the elastic deformation region and not in the plastic deformation region. However, discrepancies in axial compressive strength of high-performance fibres from different testing schemes have been noted and addressed elsewhere[17].

(5) As shown in *Table 4*, the critical compressive strains of fibres of flexible molecules (such as ABPBO and Kevlar) are always larger than those of rod-like molecules (such as PBO and PBT). However, fibres of rod-like molecules always have a superior tensile modulus.

Morphological investigation of the PBO and the ABPBO fibres involved SEM imaging as well as WAXS and SAXS. The microstructure findings are discussed below.

(1) SEM imaging was applied to examine fracture surfaces of the PBO and the ABPBO fibres. The fibre specimens were either fractured at liquid nitrogen temperature or tensile fractured at room temperature. All specimens exhibited a fibrillar structure, as detailed in *Figures 3* (ABPBO) and *4* (PBO) for fibres fractured at liquid nitrogen temperature. The fibril was as small as 0.1 μm in diameter, aligning along the fibre axial direction. No skin–core differentiation was revealed in either PBO or ABPBO fibres.

(2) WAXS on the PBO and the ABPBO fibres shows typical meridional and equatorial reflections related to

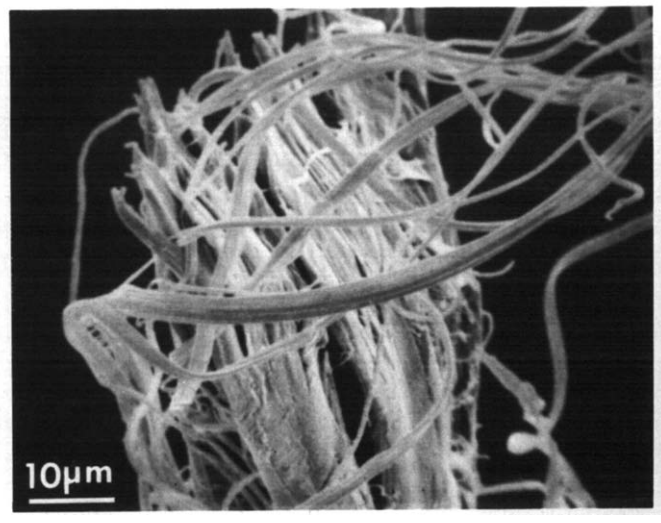

Figure 3 Scanning electron micrograph of fractured ABPBO fibre

the uniaxial nature of the fibre. The meridional reflection of a fibre reveals the repeat distance along the extended chain, and the equatorial reflection is related to the intermolecular arrangement between chains. For fibres dried under tension and/or thermally annealed, the atimuthal breadth in equatorial reflections is significantly reduced, indicating that the molecules assume an improved alignment along the fibre axis that leads to increased tensile modulus. However, a crystalline phase with three-dimensional order is less evident for the rod-like polymer PBO. It is believed that the structure of the PBO fibre is greatly influenced by its precursor in the nematic liquid-crystalline solution, i.e. the polymer has a local orientational order that can be aligned by extrusion, drawing and thermal annealing, but no positional order can be enhanced, which impedes the formation of crystallites with three-dimensional order. These morphologies are illustrated in contour plots in *Figure 5* for PBO fibres coagulated in water at 11°C, by using equal intensity of [001] reflection to normalize the scattering intensities and identical contour levels in generating the plots. The image at the centre of the contour plots is due to intensity depression from a circular beam stop. *Figure 5a* is a WAXS contour plot for the as-spun fibre dried without tension. *Figures 5b* and *c* are WAXS contour plots for the as-spun fibre dried with tensile strain of 2 and 3.6%, respectively, which display a significant decrease in azimuthal breadth of equatorial reflections for tension-dried fibres. Higher drying tensile strain generally leads to less azimuthal breadth in equatorial reflections, and to improved molecular alignment and fibre tensile modulus. Finally, *Figure 5d* is a WAXS contour plot for the 3.6% tensile-strain-dried PBO fibre heat treated at 500°C with additional tensile strain of 3.6% imposed on the fibre during the course of thermal annealing. In addition to further improvement of molecular alignment, the contour plot displays the emergence of the off-axis reflections, which suggests the formation of a three-dimensional order. For coil-like ABPBO polymer, the off-axis reflections are more pronounced in both as-spun and heat-treated fibres.

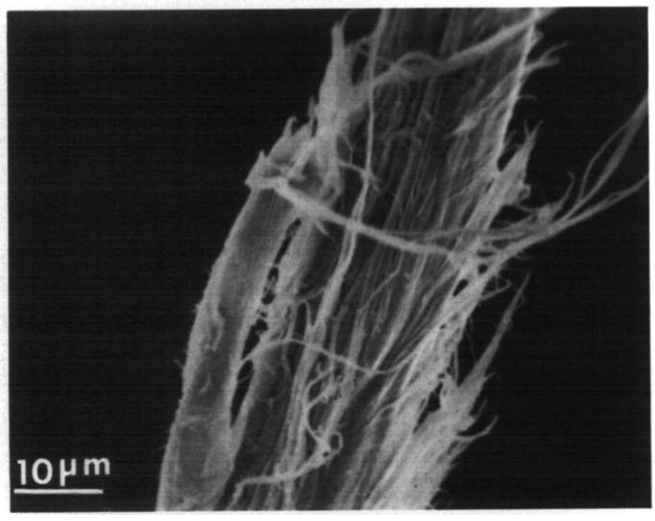

Figure 4 Scanning electron micrograph of fractured PBO fibre

SAXS on various PBO and ABPBO fibres consistently gives an anisotropic intensity pattern concentrated along the equatorial direction due to void scattering. Voids were formed during the coagulation when a drastic volume reduction occurred in leaching out the solvent, and were extended along the fibre axis under spin–draw induced elongation. The void scattering for as-spun PBO and ABPBO fibres was significantly reduced by either tension-drying or coagulation at a lower temperature. Drying of the wet filament under tension is expected to collapse voids laterally and effectively decreases the defect density of the fibre cross section; coagulation at a lower temperature would decrease the diffusion rate in leaching the PPA by H_2O, an exothermic reaction, and thus the volumetric reduction rate. Both should decrease the void content in the fibres, as evidenced in the SAXS results, and lead to enhanced tensile properties. This morphology is represented in contour plots in *Figure 6* for PBO fibres coagulated in water at 11°C, by using equal intensity of [001] reflection to normalize the scattering intensities and identical contour levels in generating the plots to allow direct comparison. *Figure 6a* is a SAXS contour plot for the as-spun PBO fibre dried without tension. *Figures 6b* and *6c* are SAXS contour plots for the as-spun fibre dried with tensile strain of 2 and 3.6%, respectively. Finally, *Figure 6d* is a SAXS contour plot for the 3.6% tensile-strain-dried PBO fibre heat-treated at 500°C with additional tensile strain of 3.6% imposed on the fibre during the course of thermal annealing. It displays less SAXS intensity from voids and also shows the emergence

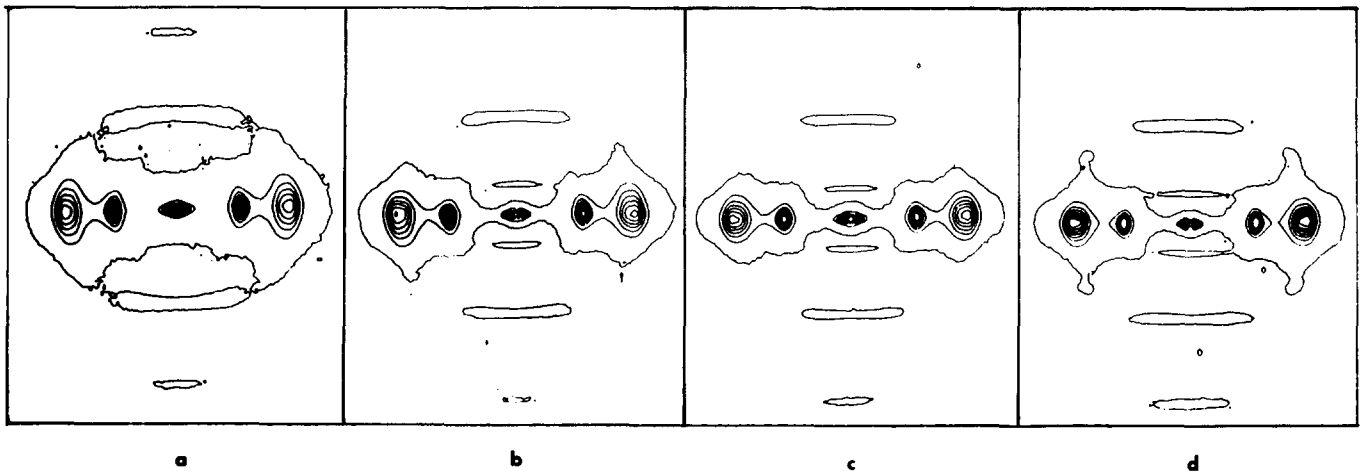

Figure 5 Contour plots of wide-angle X-ray scattering on PBO fibres coagulated with water at 11°C: (a) dried without tension; (b) dried with 2% tensile strain; (c) dried with 3.6% tensile strain and (d) then annealed at 500°C with 3.6% tensile strain

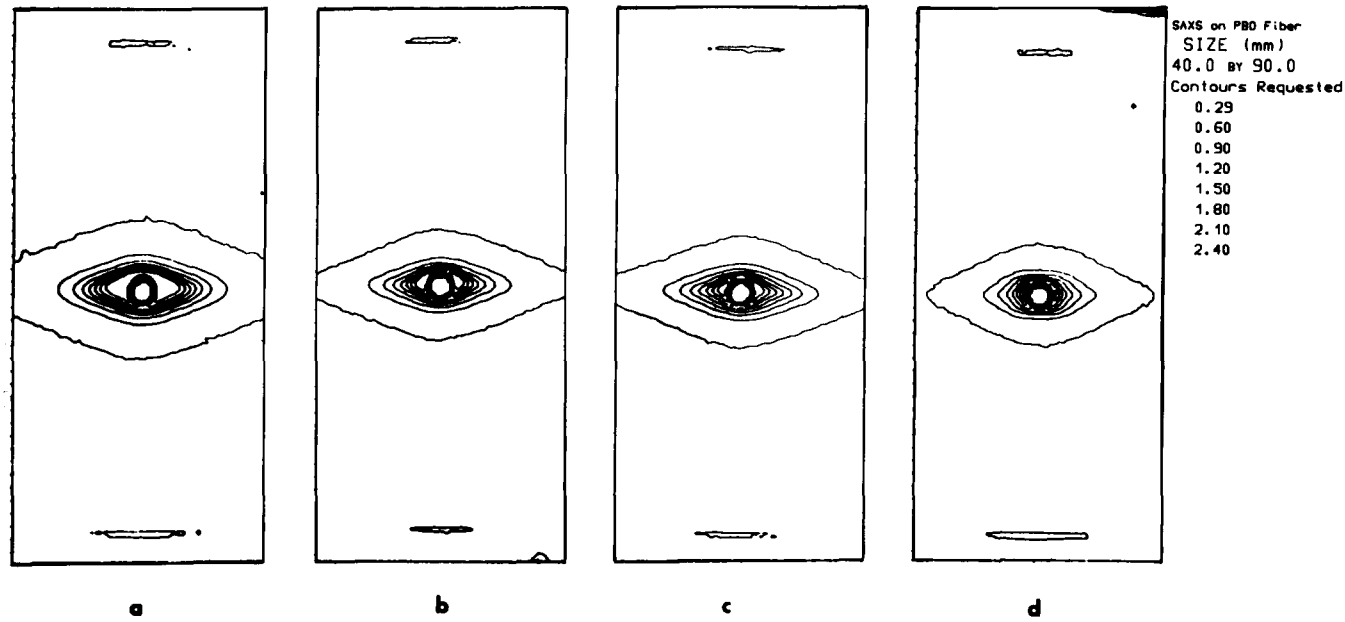

Figure 6 Contour plots of small-angle X-ray scattering on PBO fibres coagulated with water at 11°C: (a) dried without tension; (b) dried with 2% tensile strain; (c) dried with 3.6% tensile strain and (d) then annealed at 500°C with 3.6% tensile strain

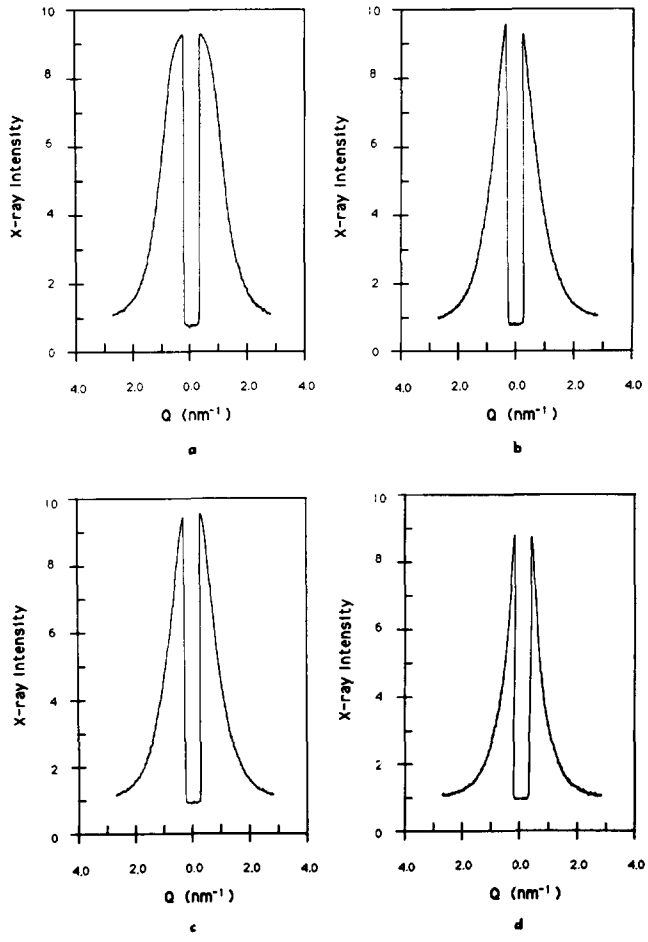

Figure 7 Equatorial intensity line scans of small-angle X-ray scattering on PBO fibres coagulated with water at 11°C: (a) dried without tension; (b) dried with 2% tensile strain; (c) dried with 3.6% tensile strain and (d) then annealed at 500°C with 3.6% tensile strain

of the off-axis reflections, indicating again an enhanced three-dimensional structural order. This off-axis radial four-point SAXS reflection becomes more pronounced with higher annealing temperatures. This is in contrast to the levelled four-point SAXS pattern usually obtained for uniaxial fibre systems. Details of this finding will be given in the following paper. The [001] reflection of the PBO fibres is also shown along the meridional direction in *Figure 6* to demonstrate the intensity normalization scheme employed for the X-ray scattering measurements. *Figures 7* and *8*, respectively, contain equatorial and meridional line scans of the SAXS intensities from the PBO fibres, showing that drying under tension or heat treatment under moderate tension reduces void scattering intensity and leads to enhanced tensile properties. Careful comparison of *Figures 6b* and *c*, or *Figures 7b* and *7c*, reveals a slight increase of the void scattering intensity as the drying strain increased from 2 to 3.6%. This excess void scattering intensity might be due to defects (voids) created in breaking the fibrillar structure by the higher drying tension. As shown in *Figure 8*, the meridional reflection at $Q = 5.2\ \text{nm}^{-1}$ is the internal standard used here for normalizing X-ray scattering intensity and is equal to the PBO repeat distance of about 1.21 nm.

CONCLUSIONS

Tensile properties of the rod-like PBO and the coil-like ABPBO fibres can be improved by coagulation at a low temperature, by tension drying and by thermal annealing. Application of tension in drying the fibres improves molecular alignment and leads to increased tensile modulus. Void content for fibres of the heteroaromatic oxazole polymers is significantly reduced by using low coagulation temperature, tension drying and thermal annealing. This also contributes to enhanced tensile properties. Thermal annealing also improves the crystallinity of the ABPBO fibre and seems to induce a three-dimensional order, which is usually absent for fibres of rod-like PBO polymer; both annealed PBO and ABPBO fibres result in a unique off-axis radial four-point SAXS pattern. The tensile modulus for fibres of rod-like polymer is normally higher than that of the coil-like polymer. However, the critical compressive strain for fibres of rod-like polymer is normally lower than that of the coil-like polymer as determined by the cantilever beam test on monofilaments.

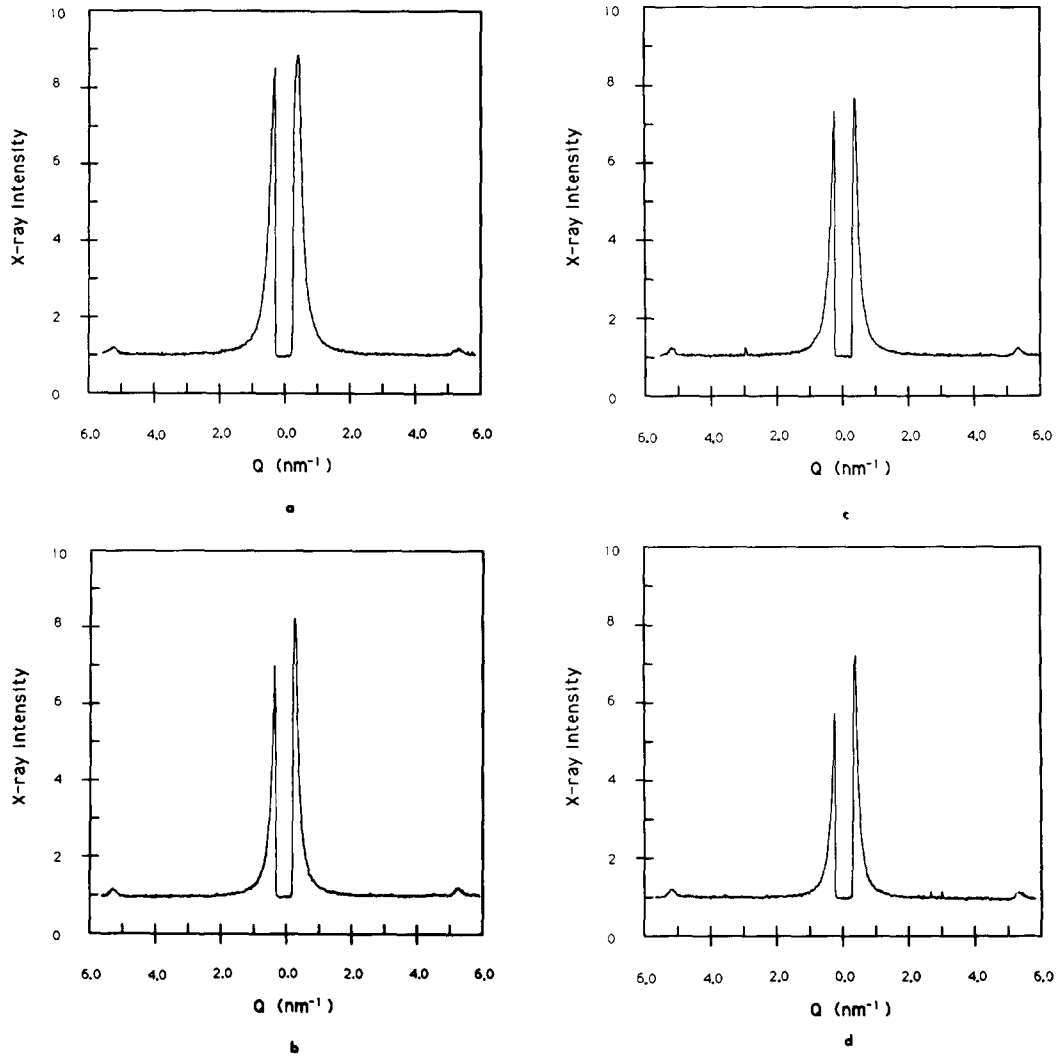

Figure 8 Meridional intensity line scans of small-angle X-ray scattering on PBO fibres coagulated with water at 11°C: (a) dried without tension; (b) dried with 2% tensile strain; (c) dried with 3.6% tensile strain and (d) then annealed at 500°C with 3.6% tensile strain

ACKNOWLEDGEMENTS

The authors thank the Air Force Materials Laboratory, Wright Research and Development Center, for supporting this study. The cantilever beam test was made by J. F. O'Brien, and morphology support was provided by C. Daily, both of the Polymer Branch, Air Force Materials Laboratory. Helpful discussion with W.-F. Hwang, currently with Dow Chemical Co., and with T. E. Helminiak, the Polymer Branch, Air Force Materials Laboratory, was most valuable and greatly appreciated.

REFERENCES

1 Moyer, Jr, W. W., Cole, C. and Anyos, T. *J. Polym. Sci. A* 1965, **3**, 2107
2 Stacey, R. D., Loire, N. P. and Levine, H. H. *Polym. Preprints* 1966, **7**, 161
3 Wolfe, J. F. and Arnold, F. E. *Macromolecules* 1981, **14**, 909
4 Wolfe, J. F., Loo, B. H. and Arnold, F. E. *Macromolecules* 1981, **14**, 915
5 Evers, R. C., Arnold, F. E. and Helminiak, T. E. *Macromolecules* 1981, **14**, 925
6 Arnold, Jr, C. *J. Polym. Sci. D* 1979, **14**, 265
7 Berry, G. C. *J. Polym. Sci. C* 1978, **65**, 143
8 Wong, C.-P., Ohnuma, H. and Berry, G. C. *J. Polym. Sci. C* 1978, **65**, 173
9 Odell, J. A., Keller, A. and Atkins, E. D. T. *Macromolecules* 1985, **18**, 1443
10 Hwang, W.-F., Wiff, D. R., Benner, C. L. and Helminiak, T. E. *J. Macromol. Sci., Phys. Edn* 1983, **B22** (2), 231
11 Hwang, W.-F., Wiff, D. R., Verschoore, C., Price, G. E., Helminiak, T. E. and Adams, W. W. *Polym. Eng. Sci.* 1983, **23**, 784
12 Welsh, W. J., Bhaumik, D. and Mark, J. E. *Macromolecules* 1981, **14**, 947
13 Wellman, M. W., Adams, W. W., Wolff, R. A., Wiff, D. R. and Fratini, A. V. *Macromolecules* 1981, **14**, 935
14 Mammone, J. F. and Uy, W. C. 'AFWAL-TR-4154 Part II', 1982
15 Sinclair, D. *J. Appl. Phys.* 1950, **21**, 380
16 Drzal, L. D. AFWAL-TR-4003, 1986
17 Allen, S. R. *J. Mater. Sci.* 1987, **22**, 853
18 Fawaz, S. A., Palazotto, A. N. and Wang, C. S. *Polymer* 1992, **33**, 100
19 Hearn, E. J. 'Mechanics of Materials: An Introduction to the Mechanics of Elastic and Plastic Deformations of Solids and Structural Components', Int. Ser. Mater. Sci. Technol., Vol. 19, Pergamon Press, New York, 1985, p. 37